

Free energy calculations of counterion partitioning between DNA and chloride solutions

 Alexey Savelyev and Garegin A. Papoian*[†]

Department of Chemistry, University of North Carolina at Chapel Hill, NC 27599-3290, USA.

E-mail: gpapoian@unc.edu

DOI: 10.1016/j.mencom.2007.03.015

The reported computational experiments provide insights into the interplay between ionic clusterization and affinity for the DNA binding while considering the competitive distribution of two similar monovalent ions, Na⁺ and K⁺, around DNA.

The condensation of monovalent counterions around DNA influences polymer properties of the DNA chain. The counterions mitigate significant electrostatic repulsion between negatively charged DNA base pairs and promote DNA compaction into highly organized structures.¹ This is exemplified by the million-fold DNA compaction into chromatin fiber in the nuclei of eukariotic cells.² The structure, stability and dynamics of the DNA chain are significantly affected by the salt buffer ionic composition.^{3,4} In particular, the distribution of two common monovalent ions, Na⁺ and K⁺, around DNA and their influence on the conformational behavior of different DNA oligomers have been studied using computational^{3–5} and experimental^{6–8} methods. However, experimental results on the relative extent of the Na⁺ and K⁺ condensation around DNA are not in complete agreement with each other.^{6–10} Recently, we found a significantly higher affinity for Na⁺ ions to condense around a 16-base-pair DNA oligomer, compared with K⁺ ions.⁵ This result is consistent with the measurement of DNA electrophoretic mobilities in various ionic buffers.⁷ In addition, another set of experiments on the compaction of long DNA chains, which is facilitated by monovalent counterions,⁸ can also be interpreted to suggest greater Na⁺ condensation.⁵ We also compared the counterion condensation details from our all-atom simulations with the predictions from the meanfield Poisson–Boltzmann theory, gaining insights into the limits of applicability of the latter approach.^{5,11}

Here we report our analysis of competitive Na⁺ vs. K⁺ condensation around DNA based on a free energy approach, as opposed to determining the ionic distribution profiles.⁵ We calculated the free energy cost of moving a K⁺ ion from a DNA solution to a bulk solution, and simultaneously, bringing a Na⁺ ion from the bulk solution to the DNA solution. The corresponding process is shown in Figure 1(a). The bulk is considered independent from the DNA solution. Thus, there are no electrostatic interactions between the polyelectrolyte and bulk solutions, which is the case in the Donnan equilibrium. The current analysis of the ionic exchange between the DNA and the bulk solutions (the latter serving as a bath with fixed ionic chemical potentials) provides important new insights into the energetics of the Na⁺ and K⁺ binding to DNA. The results are consistent with the previously found trend, namely, more favorable interactions between the Na⁺ ions and the DNA segment compared with the K⁺ ions.⁵

According to the thermodynamic cycle shown in Figure 1(b), the real physical process of ionic exchange can be represented

by two ‘alchemical’ transformations of one ion into another, in the bulk and in the vicinity of DNA, respectively. The upper horizontal leg of the cycle corresponds to the K⁺ → Na⁺ transformation in the electroneutral system **1**, which is comprised of a 16-base-pair DNA oligomer [d(CGAGGTTTAAACCTCG)]₂, neutralized by 15Na⁺ and 15K⁺ counterions, and solvated in explicit water, with additional ~0.06 M of both NaCl and KCl salts [7Na⁺ ions, 7K⁺ ions, and 14Cl⁻ ions, see Figure 1(b)]. Details on system **1** preparation and parameterization can be found in the Online Supplementary Materials section (see also ref. 5). The K⁺ → Na⁺ transformation results in a new salt composition of 8Na⁺ and 6K⁺ ions and the free energy change $\Delta G_{K^+ \rightarrow Na^+}^{DNA}$. Next, we consider the lower horizontal leg of the thermodynamic cycle in Figure 1(b), which reflects the reverse Na⁺ → K⁺ transformation in the bulk system **2**, which was obtained from system **1** by removing DNA and its neutralizing counterions. This process produces a new salt composition of 6Na⁺ and 8K⁺ ions [see Figure 1(b)] with the free energy difference $\Delta G_{Na^+ \rightarrow K^+}^{bulk} = -\Delta G_{K^+ \rightarrow Na^+}^{bulk}$. The difference between the free energy changes computed in systems **1** and **2**, $\Delta \Delta G$, represents the free energy cost of the real process, the exchange of one Na⁺ and one K⁺ ions between the DNA and bulk solutions.

To compute $\Delta G_{Na^+ \rightarrow K^+}^{bulk}$ and $\Delta G_{K^+ \rightarrow Na^+}^{bulk}$ we used the standard thermodynamic integration (TI) technique,¹²

$$\Delta G \equiv G(\lambda = 1) - G(\lambda = 0) = \int_0^1 d\lambda \left\langle \frac{\partial H(\lambda)}{\partial \lambda} \right\rangle.$$

The transformation Hamiltonian is represented as

$$H(\lambda) = H_1 + \lambda(H_2 - H_1),$$

where H_1 and H_2 correspond to the initial and final states, respectively. The coupling parameter $\lambda \in [0, 1]$ continuously morphs the initial state into the final state. In particular, the initial and final states of system **1** correspond to the 7Na⁺/7K⁺ and 8Na⁺/6K⁺ salt compositions, respectively. In the bulk system **2**, the initial and final states correspond to the 7Na⁺/7K⁺ and 6Na⁺/8K⁺ ionic compositions, respectively [see Figure 1(b)].

We used a five-point Gaussian quadrature to numerically compute the integral

$$\int_0^1 d\lambda \left\langle \frac{\partial H(\lambda)}{\partial \lambda} \right\rangle.$$

The averages $\langle \partial H(\lambda) / \partial \lambda \rangle_{\lambda_i}$, corresponding to different values of λ_i , $i = 1..5$, were collected from a series of extensive all-atom MD simulations of systems **1** and **2**. These simulations were carried out using the Sander module of the AMBER package¹³ and the AMBER Parm99 force field.¹⁴ Systems **1** and **2** were

[†] A former student of the Higher Chemical College of the RAS (1990–1994).

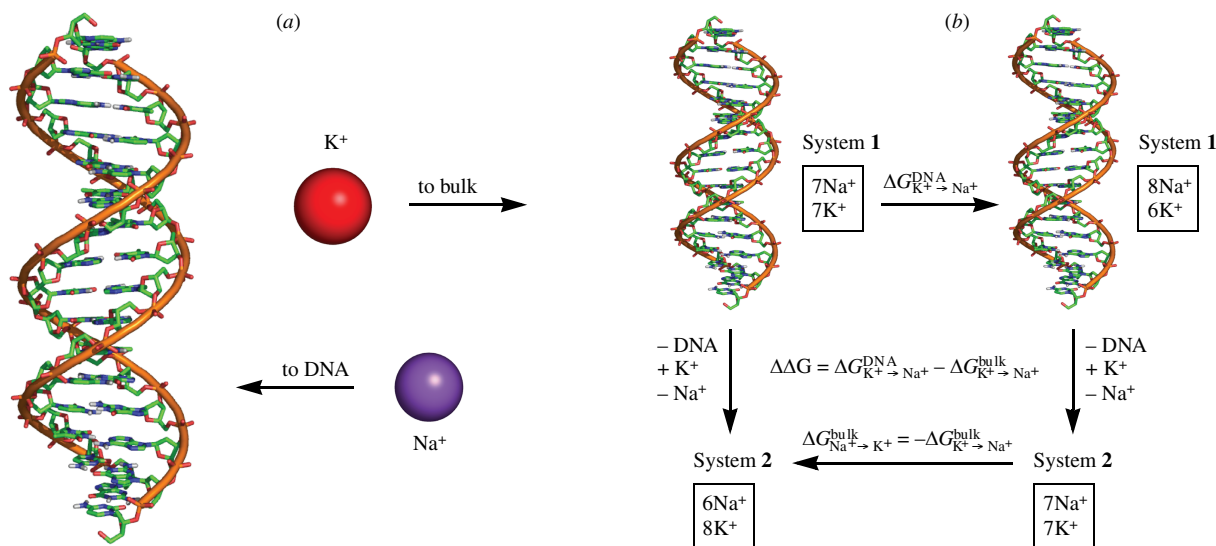


Figure 1 The real process of moving the K^+ ions away from DNA to the bulk phase, accompanied by approaching the Na^+ ion to DNA from the bulk (a), can be represented by two artificial processes (b): transformation of K^+ ion into Na^+ ion at the DNA proximity in the system 1 (upper black leg of thermodynamic cycle) and the reverse $Na^+ \rightarrow K^+$ transformation in the bulk system 2, away from DNA (lower black leg of thermodynamic cycle). The double free energy difference between two legs, $\Delta\Delta G = \Delta G_{K^+ \rightarrow Na^+}^{DNA} - \Delta G_{K^+ \rightarrow Na^+}^{bulk}$, is the value of interest. Alternatively, the process may be described by the $-DNA - Na^+ + K^+$ transformation of system 1, having different initial salt compositions (see vertical arrows).

first equilibrated for 60 and 30 ns, respectively (additional details are provided in the Online Supplementary Materials section). A series of five equilibration runs, corresponding to λ_i , $i = 1..5$, were carried out for 6 ns followed by 10 ns and production runs. The MD simulations reported here were run for a combined time of $\sim 0.2 \mu s$, making them among the most extensive all-atom explicit solvent MD simulations of DNA. The values of $\Delta G_{K^+ \rightarrow Na^+}^{DNA}$, $\Delta G_{Na^+ \rightarrow K^+}^{bulk}$ and $\Delta\Delta G$ as a function of simulation time are suggestive of convergence after approximately 6 ns, indicating sufficient equilibration and production times.

The obtained result of $\Delta\Delta G \approx 0$ is surprising since the Na^+ ions were shown to condense twice as strongly around DNA than the K^+ ions, in competitive binding simulations.⁵ To explain this discrepancy, we hypothesize that remarkably different interactions between the Cl^- coions and the Na^+ and K^+ counterions may produce a compensatory contribution to the free energy of the $Na^+ \rightarrow K^+$ transformation. We found previously that K^+ and Cl^- form constantly broken and re-formed K^+-Cl^- clusters comprised of several K^+ and Cl^- ions.⁵ Almost half of all K^+ ions ($\sim 45\%$) in the course of MD simulation have been found associated in clusters of different sizes and compositions.

Table 1 Free energy changes (kcal mol^{-1}) computed in systems 1 and 2 every 2 ns of production run. The approximately 17 kcal mol^{-1} computed for the $Na^+ \rightarrow K^+$ transformations in 2 agrees well with the experimental value of 16 kcal mol^{-1} obtained from solutions in a standard state.²⁰

| | $\Delta G_{K^+ \rightarrow Na^+}^{DNA}$ | $\Delta G_{Na^+ \rightarrow K^+}^{bulk}$ | $\Delta\Delta G$ |
|-------|---|--|------------------|
| 2 ns | -17.3477 | 17.1232 | -0.2245 |
| 4 ns | -17.2747 | 17.2591 | -0.0157 |
| 6 ns | -17.2623 | 17.3084 | 0.0461 |
| 8 ns | -17.2036 | 17.1398 | -0.0638 |
| 10 ns | -17.2068 | 17.2240 | 0.0172 |

Table 2 Free energy changes (kcal mol^{-1}) computed in modified systems 1 and 2 every 2 ns of production run. The approximately 16 kcal mol^{-1} computed for the $Na^+ \rightarrow K^+$ transformations in 2 agrees well with the experimental value of 16 kcal mol^{-1} obtained from solutions in a standard state.²⁰

| | $\Delta G_{K^+ \rightarrow Na^+}^{DNA}$ | $\Delta G_{Na^+ \rightarrow K^+}^{bulk}$ | $\Delta\Delta G$ |
|-------|---|--|------------------|
| 2 ns | -17.5276 | 15.0571 | -2.4730 |
| 4 ns | -17.4815 | 16.2823 | -1.1993 |
| 6 ns | -17.4731 | 16.3582 | -1.1148 |
| 8 ns | -17.4740 | 16.1952 | -1.2788 |
| 10 ns | -17.4607 | 16.1707 | -1.2900 |

In contrast, the extent of the formation of similar Na^+-Cl^- clusters was negligible.⁵ Thus, $\Delta\Delta G \approx 0$ may result from the cancellation of two opposing contributions: (1) a free energy gain resulting from the stronger tendency of Na^+ to interact with DNA and (2) a free energy loss because of diminished K^+-Cl^- cluster formation in the bulk compared to the DNA solution, since the locally enhanced K^+ concentration near DNA (due to the counterion condensation effect) results in strong K^+-Cl^- clusterization.⁵

To verify this hypothesis, we modified systems 1 and 2 and then repeated all MD simulations and calculated free energy changes of the same ionic transformations. The modifications were the following: in system 1, we removed extra salt ($7Na^+$, $7K^+$ and $14Cl^-$ ions), leaving $15Na^+$ and $15K^+$ neutralizing ions. In this way, we excluded the possibility of cluster formation. System 2 was then comprised of $15Na^+$, $15K^+$ and $30Cl^-$ ions. Note that the numbers of Na^+ and K^+ ions are equal in both systems (15 of each); however, the source of a negative charge (-30) is the polyelectrolyte (DNA) in system 1 and the electrolyte, or $30Cl^-$ ions, in system 2. Such a construction of modified systems 1 and 2 allows us to ‘decouple’ two energetic contributions mentioned above. The data shown in Table 2 indicate convergence after 6 ns of production runs. The average $\Delta\Delta G = -1.24 \text{ kcal mol}^{-1}$ corresponds to $\approx 2k_B T$, indicating that in the modified systems the concentrations of Na^+ and K^+ ions near the DNA and in the bulk, respectively, would noticeably differ. Specifically, the Na^+ ions will be preferentially enriched near DNA, in agreement with our prior conclusions. However, if a salt is added to the DNA-counterion system, the K^+-Cl^- clusterization acts to stabilize the K^+ ions, resulting in $\Delta\Delta G \approx 0$ obtained in the first set of free energy simulations.

To verify whether the obtained results are force-field specific, we repeated a simulation of system 1 utilizing the Charmm27 force-field,^{15,16} which, along with Amber, is among the most commonly used all-atom force-fields. In particular, we analyzed the Na^+ vs. K^+ distribution around the DNA oligomer and also studied the coion-counterion cluster formation. Although the K^+-Cl^- association is much less pronounced in Charmm (only $\sim 5\%$ of K^+ , compared to $\sim 45\%$ of K^+ in Amber, participate in clustering), Na^+ ions are still condensed around DNA to a larger degree compared to K^+ . We have found that in the vicinity of DNA (within the Manning radius of $\sim 9 \text{ \AA}$ from polyion surface¹⁷)

Na⁺ prevails by ~7% in Charmm, whereas this domination is further enhanced to ~25% in Amber. The diminution of the DNA selectivity towards different ionic species, as well as a significant decrease in the extent of K⁺–Cl[–] clustering, as one replaces Amber by Charmm, may be attributed to dissimilar parameters in the corresponding Lennard–Jones potentials for ions. Indeed, it is natural to assume that a smaller ionic radius of K⁺ in Charmm makes unfavorable the association with (also smaller) Cl[–] due to an increase in dehydration penalty. Despite that, however, both force-fields accurately reproduce the available experimental data on the Na⁺/water and K⁺/water radial distribution functions, as well as the free energies of ionic hydration in aqueous NaCl and KCl solutions.^{18,19} Thus, the incomplete agreement between Charmm and Amber results reflects the lack of the broader experimental knowledge about the structural and energetic properties of ionic aqueous solutions. The question of what force-field is more suitable, or ‘correct’, for addressing the problem of counterion condensation cannot be fully addressed at this point.

The above brief comparison between the Amber and Charmm simulation results might indicate that the extent of the K⁺–Cl[–] association could be overestimated in Amber, while it could be underestimated in Charmm. In that case, the clustering behaviour of a dilute KCl solution would be intermediate between these predictions. A more systematic comparison of Amber and Charmm force-fields, in the context of analyzing the competitive ionic binding to DNA, will be published elsewhere. In summary, the reported computational experiments provide insights into the interplay between ionic clusterization and affinity for the DNA binding while considering the competitive distribution of two similar monovalent ions, Na⁺ and K⁺, around DNA.

Online Supplementary Materials

Supplementary data associated with this article can be found in the online version at doi:10.1016/j.mencom.2007.03.015.

References

- 1 W. Saenger, *Principles of Nucleic Acid Structure*, Springer, New York, 1984.
- 2 B. Alberts, A. Johnson, J. Lewis, M. Raff, K. Roberts and P. Walter, *Molecular Biology of the Cell*, Garland Science, New York and London, 2002.
- 3 A. P. Lyubartsev and A. Laaksonen, *J. Biomol. Struct. Dyn.*, 1998, **16**, 579.
- 4 P. Varnai and K. Zakrzewska, *Nucleic Acids Res.*, 2004, **32**, 4269.
- 5 A. Savelyev and G. A. Papoian, *J. Am. Chem. Soc.*, 2006, **128**, 14506.
- 6 V. P. Denisov and B. Halle, *Proc. Natl. Acad. Sci. USA*, 2000, **97**, 629.
- 7 E. Stellwagen, Q. Dong and N. C. Stellwagen, *Biopolymers*, 2005, **78**, 62.
- 8 A. A. Zinchenko and K. Yoshikawa, *Biophys. J.*, 2005, **88**, 4118.
- 9 N. Korolev, A. P. Lyubartsev, A. Rupprecht and L. Nordenskiöld, *Biophys. J.*, 1999, **77**, 2736.
- 10 N. Korolev, A. P. Lyubartsev, A. Rupprecht and L. Nordenskiöld, *Biopolymers*, 2001, **58**, 268.
- 11 L. Guldbrand, B. Jonsson, H. Wennerstrom and P. Linse, *J. Chem. Phys.*, 1984, **80**, 2221.
- 12 D. Frenkel and B. Smit, *Understanding Molecular Simulation*, Academic Press, San Diego, 1996.
- 13 D. Case, T. Cheatham, T. Darden, H. Gohlke, R. Luo, K. Merz, A. Onufriev, C. Simmerling, B. Wang and R. Woods, *J. Comput. Chem.*, 2005, **26**, 1668.
- 14 J. Wang, P. Cieplak and P. Kollman, *J. Comput. Chem.*, 2000, **21**, 1049.
- 15 A. MacKerell, N. Banavali and N. Foloppe, *Biopolymers*, 2001, **56**, 257.
- 16 B. R. Brooks, R. E. Bruccoleri, B. D. Olafson, D. J. States, S. Swaminathan and M. Karplus, *J. Comput. Chem.*, 1983, **4**, 187.
- 17 G. S. Manning, *J. Chem. Phys.*, 1969, **51**, 924.
- 18 M. Patra and M. Karttunen, *J. Comput. Chem.*, 2004, **25**, 678.
- 19 M. Cavallari, C. Cavazzoni and M. Ferrario, *Mol. Phys.*, 2004, **102**, 959.
- 20 R. A. Robinson and R. H. Stokes, *Electrolyte Solutions*, Dover, New York, 2002.

Received: 1st November 2006; Com. 06/2808